Acta Crystallographica Section D
Biological Crystallography
ISSN 0907-4449

An alternate binding site for the P1–P3 group of a class of potent HIV-1 protease inhibitors as a result of concerted structural change in the 80s loop of the protease

Sanjeev Munshi,* Zhongguo Chen, Youwei Yan, Ying Li, David B. Olsen, Hilary B. Schock, Brendan B. Galvin, Bruce Dorsey and Lawrence C. Kuo

Department of Antiviral Research, Merck Research Laboratories, West Point, PA 19486, USA

Correspondence e-mail: sanjeev_munshi@merck.com

Received 21 September 1999
Accepted 6 January 2000

PDB References: 9X mutant HIV-1 protease–Indinavir complex, 1c6y; wild-type HIV-1 protease–L-756,423 complex, 1c70; 9X mutant HIV-1 protease–L-739,622 complex, 1c6x; 9X mutant HIV-1 protease–Saquinavir complex, 1c6z.

Structures of the complexes of HIV protease inhibitor L-756,423 with the HIV-1 wild-type protease and of the inhibitors Indinavir, L-739,622 and Saquinavir with the mutant protease (9X) containing nine point mutations (Leu10Val, Lys20Met, Leu24Ile, Ser37Asp, Met46Ile, Ile54Val, Leu63Pro, Ala71Val, Val82Thr) have been determined. Comparative analysis of these structures reveals an alternate binding pocket for the P1–P3 group of Indinavir and L-756,423. The alternate binding pocket is a result of concerted structural change in the 80s loop (residues 79–82) of the protease. The 80s loop is pulled away from the active site in order to accommodate the P1–P3 group, which is sandwiched between the flap and the 80s loop. This structural change is observed for the complexes of the wild type as well as the 9X mutant protease. The study reveals that the 80s loop is an intrinsically flexible loop in the wild-type HIV-1 protease and that mutations in this loop are not necessary to result in conformational changes. Conformation of this loop in the complex depends primarily upon the nature of the bound inhibitor and may be influenced by mutations in the protease. The results underscore the need to understand the intrinsic structural plasticity of the protease for the design of effective inhibitors against the wild-type and drug-resistant enzyme forms. In addition, the alternate binding pocket for the P1–P3 group of Indinavir and L-756,423 may be exploited for the design of potent inhibitors.

1. Introduction

The remarkable success of HIV-1 protease inhibitors as antiretroviral agents has provided tremendous impetus for developing more efficacious inhibitors. Clinical regimens containing the currently available protease inhibitors are potent enough to drive viral load to undetectable levels in HIV-positive patients (Gulick *et al.*, 1997, 1998). However, the emergence of variants of HIV isolates that are resistant to protease inhibitors continues to be a hurdle in combating AIDS (Condra, 1998; Boden & Markowitz, 1998). One of the phenotypic manifestations of resistance is the selection of virus that contains mutations in the amino-acid sequence of the protease. A large number of amino-acid residues in the protease molecule have been implicated in conferring varying degrees of resistance to protease inhibitors (Condra *et al.*, 1996; Molla *et al.*, 1996; Patick *et al.*, 1996). Since HIV protease functions as a dimer, any single amino-acid change at the genetic level appears twice in its functional form. These mutations can be mapped to the active site (inhibitor/substrate-binding site) as well as away from the active site (Carroll & Kuo, 1998; Condra, 1998; Boden & Markowitz, 1998). Mutations are observed against all therapeutic regi-

mens of different protease inhibitors approved by the FDA. Amino-acid substitutions in the mutant protease may be inhibitor-specific, although the ever-growing database of the variants of HIV found in patients that are resistant to treatment with different protease inhibitors (currently approved by the FDA) seems to reflect significant cross-resistance pattern (Condra *et al.*, 1996; Tisdale *et al.*, 1995; Smith & Swanstrom, 1996; Olsen *et al.*, 1999).

X-ray crystal structures of a number of different complexes of the wild-type and mutant protease molecules bound to a specific inhibitor have been elucidated in order to understand the structural basis for the development of resistance (Wlodawer & Vondrasek, 1998; Wlodawer & Erickson, 1993; Chen *et al.*, 1994; Baldwin *et al.*, 1995; Abdel-Meguid *et al.*, 1994; Ala *et al.*, 1998; Hoog *et al.*, 1996; Swairjo *et al.*, 1998; Ridky *et al.*, 1998). These studies have primarily been helpful in rationalizing the influence of active-site mutations that are in direct contact with the inhibitor. In a few of these examples, structural changes observed between the wild-type and mutant protease–inhibitor complexes have been consistent with the kinetic studies (Baldwin *et al.*, 1995; Priestle *et al.*, 1995; Chen *et al.*, 1995). Conformational changes in the main-chain atoms of residues 80–84 have been observed in the complex of mutant (Val82Ala) HIV-1 protease with inhibitor A-77003 (Baldwin *et al.*, 1995). Similar structural changes have been recognized by comparing the structures of complexes of HIV-1 and HIV-2 proteases with certain inhibitors containing bulky P1 groups (Priestle *et al.*, 1995; Mulichak *et al.*, 1993). Structural changes in the 80s loop in both subunits have also been reported in the structures of the chimeras of HIV-1 protease and SIV protease bound to inhibitor SB203386 (Hoog *et al.*, 1996; Swairjo *et al.*, 1998). The structural changes in the 80s loop in the reported examples have been implied to be a consequence of the differences in the amino-acid sequence at position 82 between the proteases of HIV-1 and HIV-2/SIV and have been implicated to be responsible for differences in ligand binding to these proteases (Stebbins *et al.*, 1997).

Compared with the inhibitors with bulky P1 groups, Indinavir (I) has a smaller P1 (piperazine) group (Fig. 1). In the crystal structures of the complexes of (I) with HIV-1 and HIV-2 protease, no significant main-chain conformational differences are observed between the two structures, despite the presence of Ile at position 82 in the HIV-2 protease. Similarly, no significant conformational changes in the 80s loop are observed between the complexes of (I) with wild-type

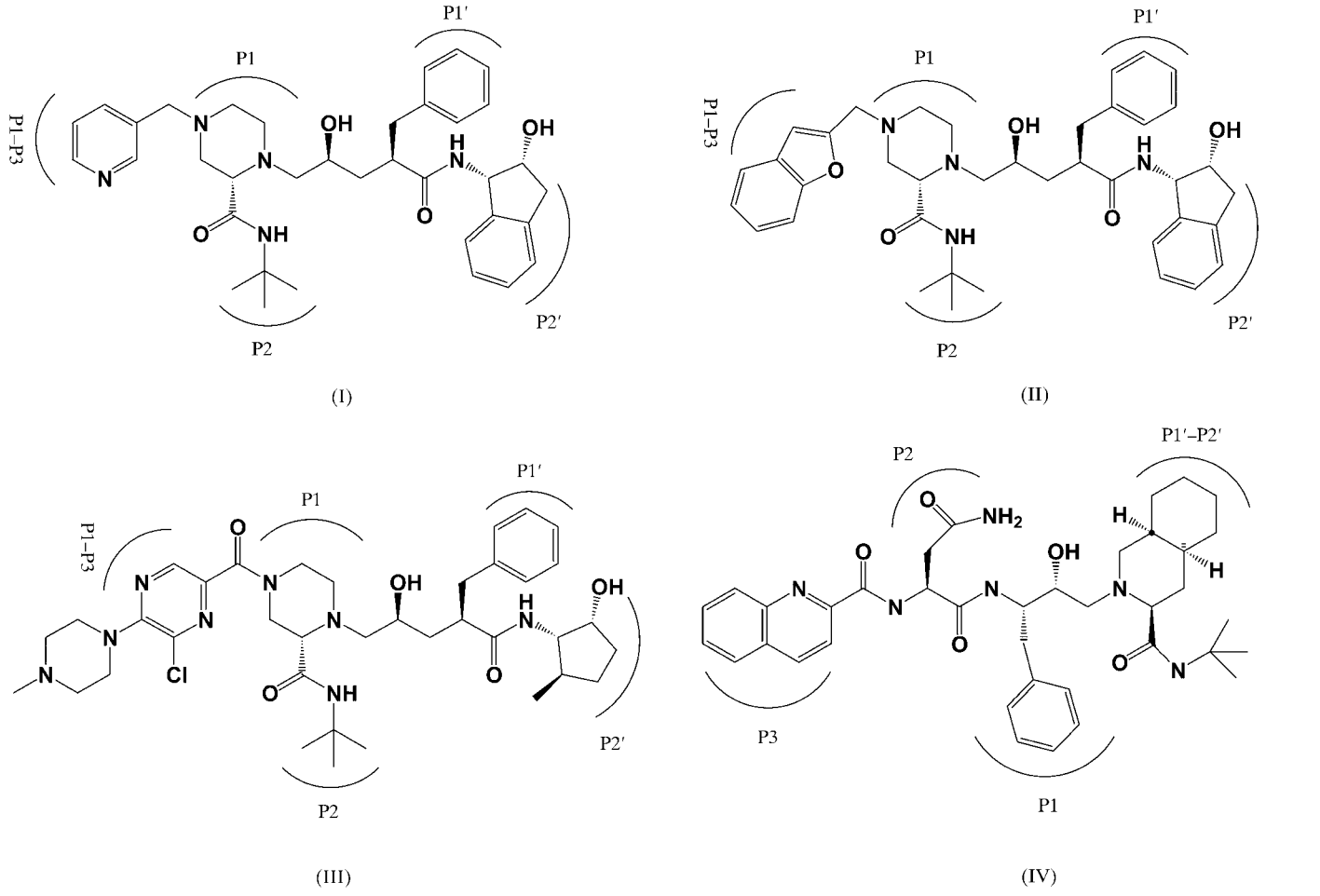

Figure 1
Chemical structures of the HIV-1 protease inhibitors used in the present studies. (I) Indinavir; (II) L-756,423; (III) L-739,622; (IV) Saquinavir.

and 4X mutant of HIV-1 protease containing four mutations (Met46Ile, Leu63Pro, Val82Thr, Ile84Val; Chen *et al.*, 1995; Schock *et al.*, 1996). Thus, it is not apparent that the complexes of (I) or its analogs would involve any significant main-chain rearrangement upon binding to HIV-1 protease and/or its drug-resistant forms.

Towards our goal of understanding the structural basis for the design of potent protease inhibitors against the wild-type and perhaps a broad spectrum of protease mutants, we have carried out X-ray crystallographic studies of a number of potent inhibitors complexed with the wild-type as well as a 9X mutant of HIV-1 protease. The 9X mutant protease is a clinically derived variant of HIV-1 protease that contains nine point mutations (Leu10Val, Lys20Met, Leu24Ile, Ser37Asp, Met46Ile, Ile54Val, Leu63Pro, Ala71Val, Val82Thr). We report the structures of the complexes of L-756,423 (II) with the wild-type HIV-1 protease and those of (I), L-739,622 (III) and Saquinavir (IV) with the 9X protease. Comparison of these structures together with the structures of the complexes of (I) with the wild-type HIV-1 and HIV-2 enzymes (Chen *et al.*, 1994) offers information regarding the conformational flexibility in the main-chain of the 80s loop of the HIV-1 protease. Understanding of the intrinsic conformational flexibility of the HIV protease is underscored by the current ongoing efforts to design potent inhibitors to combat the emergence of protease-inhibitor resistant viral isolates.

2. Materials and methods

2.1. Preparation of the HIV-1 (wild-type) and 9X mutant protease

Wild-type HIV-1 protease was purified using the protocol described (Chen *et al.*, 1994). The cloning, expression, purification and characterization of the 9X mutant protease has been described previously (Olsen *et al.*, 1999).

2.2. Crystallization of protein–inhibitor complexes

Crystals of all the complexes with either the HIV-1 wild type or 9X mutant protease were obtained as described previously (Chen *et al.*, 1994, 1995; Munshi *et al.*, 1998). The enzyme concentration used varied between 4 and 6 mg ml^{-1} in 10 m*M* MES pH 5.0, 1 m*M* DTT, 1 m*M* EDTA, 3 m*M* NaN_3. The reservoir solution contained 0.6–0.8 *M* NaCl and 0.1 *M* NaOAc pH 5.2. Inhibitors were dissolved in 100% DMSO and mixed with the protein containing buffer in a molar ratio of 1:3 to 1:5, with a final DMSO concentration of 2–5%. The inhibitor–protein mixture and the reservoir solution were mixed in a 1:1(*v*/*v*) ratio to set up hanging drops of 6–8 µl. Crystals appeared within 24 h and grew to full size in a week. Crystals of the complex of the wild-type protease with (II) and that of 9X protease with (I) appeared as thin orthorhombic plates or, occasionally, rods and are similar to those reported for the complex of the wild-type protease with (I) (Chen *et al.*, 1994). Morphology of the crystals of the complexes of (III) and (IV) with 9X protease suggested a tetragonal crystal form.

Table 1
Data acquisition and structure-refinement statistics.

A, complex of 9X mutant HIV-1 protease with (I); *B*, complex of wild-type HIV-1 protease with (II); *C*, complex of 9X mutant HIV-1 protease with (III); *D*, complex of 9X mutant HIV-1 protease with (IV).

	A	*B*	*C*	*D*
Space group	$P2_12_12$	$P2_12_12$	$P2_12_12_1$	$P2_12_12_1$
Unit-cell parameters				
a (Å)	58.44	59.86	88.20	88.13
b (Å)	88.26	87.12	88.19	88.14
c (Å)	42.94	46.97	32.92	32.99
Resolution limits (Å)	20–2.5	20–2.5	20–2.5	20–2.5
No. of observations, $I/\sigma(I) \geq 0.0$				
Total	35099	33787	79495	41654
Unique	7254	7292	8318	7717
R_{sym}† (%)	5.2	7.4	5.1	6.2
Completeness (%)	89.1	86.0	88.2	81.8
Highest resolution bin				
Resolution limits (Å)	2.59–2.5	2.59–2.5	2.59–2.5	2.59–2.5
Completeness (%)	84.2	78.5	84.0	73.2
$I/\sigma(I)$	4.4	1.8	4.5	4.0
Total observations	1775	1291	2887	2345
Unique reflections	676	648	775	677
R_{sym} (%)	16.5	28	16.7	22.4
Refinement resolution range (Å)	8.0–2.5	8.0–2.5	8.0–2.5	8.0–2.5
Crystallographic *R* factor‡ (%)	18.8	16.4	20.4	18.8
R_{free}§ (%)	31.5	27.1	30.8	29.6
RMSD bonds (Å)	0.017	0.012	0.015	0.017
RMSD angles (°)	2.1	2.8	2.4	2.5
Number of non-H atoms				
Protein	1514	1514	1514	1514
Inhibitor	45	48	37	49
Water molecules	85	107	69	76

† $R_{sym} = 100 \times [\sum\sum|\langle I(h)\rangle - I(h)i|]/\sum I(h)i$, where $I(h)i$ is the ith observation of reflection h and $\langle I(h)\rangle$ is the mean intensity of all observations of h. ‡ *R* factor $= 100 \times \big[\big||F_{obs}(h)| - |F_{calc}(h)|\big|\big]/\sum|F_{obs}(h)|$, where $F_{obs}(h)$ and $F_{calc}(h)$ are the observed and calculated (final structure) structure-factor amplitudes, respectively. Reflections with $|F| \geq 2.0\sigma$ were used for refinement. § 8–10% of the reflections were used for calculating R_{free}.

2.3. Data collection and processing

X-ray diffraction data for all the complexes were collected at ambient temperature on an R-AXIS II imaging-plate system using Cu $K\alpha$ radiation from a rotating-anode source (Rigaku RU-200 operating at 50 kV and 100 mA) focused with a double-mirror system. The data were processed and scaled using the programs *DENZO* and *SCALEPACK* from the *HKL* suite (Otwinowski & Minor, 1997). Data statistics are summarized in Table 1.

Crystals of the complexes of 9X mutant protease with (I) and those of wild-type protease with (II) belong to the $P2_12_12$ space group. Crystals of the complexes of (III) and (IV) with 9X protease were initially accepted as belonging to the 4/*m* Laue group, as the unit-cell constants *a* and *b* are identical and the acceptable V_m value (Matthews, 1968) would allow four protease dimer molecules in the unit cell. Laue group 4/*mmm* was ruled to be unlikely because of the unit-cell volume and the asymmetric nature of the bound inhibitor. Analysis of the

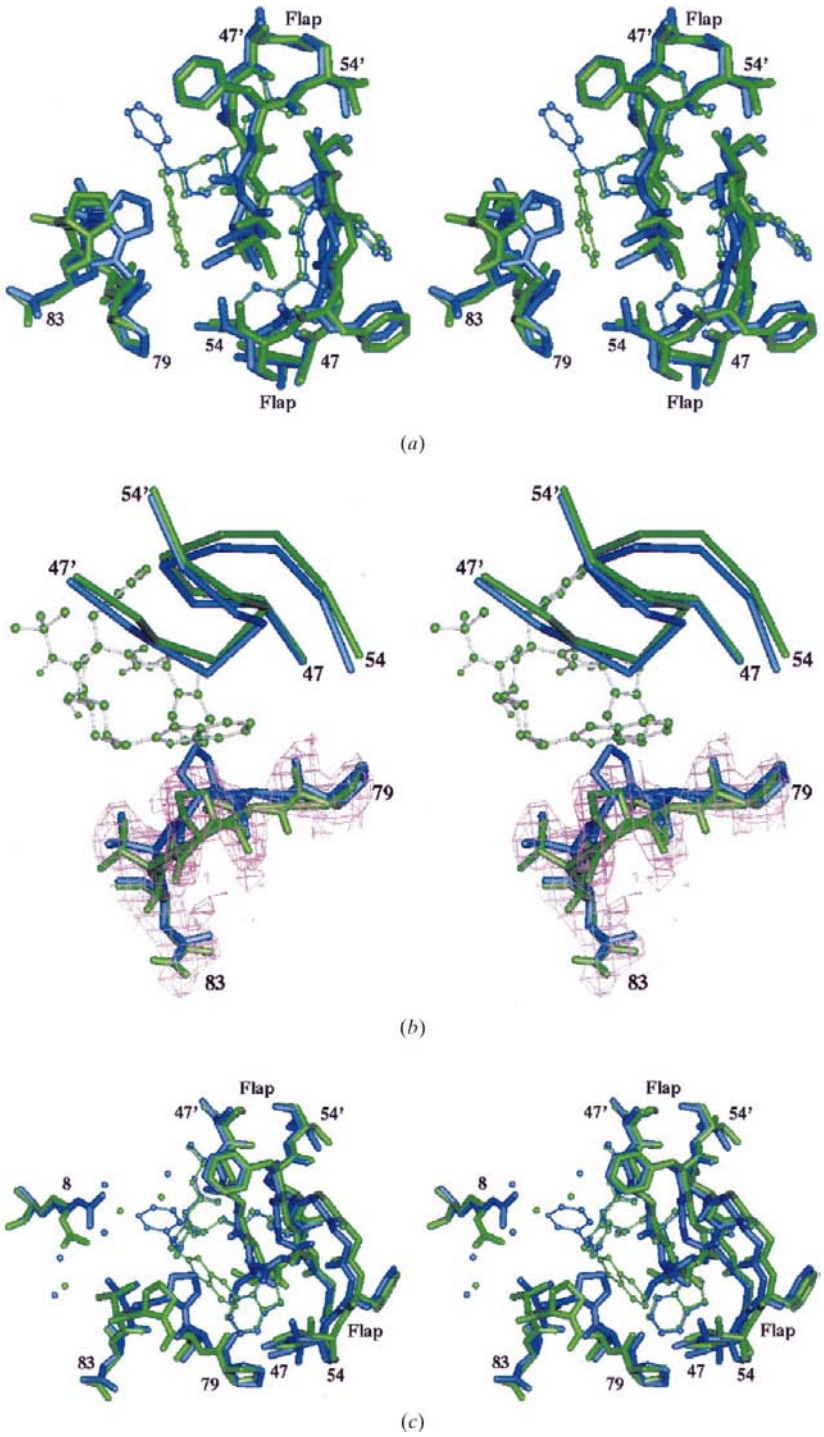

Figure 2
Superposition of the crystal structures of wild-type HIV-1 protease complexed with (I) (blue) and (II) (green). The 80s loop, comprised of residues 79–83, and the flap residues 47–54 of the two monomers are depicted. The inhibitor structures are represented as ball-and-stick models. (*a*) The P1–P3 (benzofuran) of (II) is sandwiched between the 80s loop and the flap. Pro81 is pulled away by 2.0 Å in order to accommodate the P1–P3 group. (*b*) The $2|F_o| - |F_c|$ map contoured at 1.0σ represents the electron density for the 80s loop in the complex of wild-type protease with (II). The map was computed using phases from the initial protein model without any inhibitor (blue) which had been optimized by rigid-body refinement. The final refined model of the 80s loop and the inhibitor (II) are depicted in green. (*c*) The P1–P3 (pyridyl group in blue) of (I) interacts with Arg8 and is exposed to solvent. In contrast, the P1–P3 (benzofuran group in green) of (II) is sandwiched between the 80s loop and the flap and does not interact with Arg8. Instead, Arg8 interacts with the water molecules, represented as colored dots.

systematic absences, however, suggested the likely space group to be $P2_12_12_1$, despite the unit-cell constants *a* and *b* being identical. Scaling the data using the *mmm* or 4/*m* Laue symmetry resulted in similar residuals for the symmetry-related reflections.

2.4. Structure determination

Structures of the complexes of the 9X mutant or the wild-type protease with inhibitors (I)–(IV) were determined by direct refinement. The previously determined structure of the complex of (I) with wild-type HIV-1 protease in the $P2_12_12$ space group (Chen *et al.*, 1994) was used as the phasing model for the complexes of (I) with 9X mutant and (II) with wild-type protease. The structure of the complex of L-840,236 with 9X mutant protease was determined in the space group $P2_12_12_1$ (data not shown). These coordinates were used for the structure determination of the complexes of 9X mutant protease with (III) and (IV). Rigid-body refinement of the protein dimer was followed by molecular-dynamics refinement using the program *X-PLOR* (Brünger, 1993; Table 1). The inhibitor was modeled into the difference Fourier ($|F_o| - |F_c|$) electron-density map and the ordered solvent molecules were subsequently incorporated into the model. For the 9X mutant protease structures, all nine amino-acid substitutions were represented as Gly in both subunits of the phasing model. Appropriate amino-acid side chains were incorporated after building and refining the bound inhibitor conformation.

3. Results

3.1. Structure of the wild-type HIV-1 protease–inhibitor complex

In the structure of the complex of (I) with HIV-1 or HIV-2 wild-type protease, the S1–S3 binding site is primarily lined by residues Arg8 and Gly48. The P1–P3 group of (I) points towards the solvent and makes a weak hydrogen bond with the guanidinium group of Arg8. (II), being an analog of (I), is expected to bind in a similar fashion. However, the crystal structure of (II) with the wild-type HIV-1 protease reveals an unexpected binding mode for the P1–P3 benzofuran group. This group is flipped up to be sandwiched between the flap and the 80s loop (residues 79–82; Figs. 2*a* and 2*b*). In order to accommodate the inhibitor, the

main-chain atoms of the 80s loop of one monomer undergo a conformational change, moving as much as 2.0 Å away from the active site. As a result, an alternate S1–S3 binding site is revealed. This S1–S3 binding site is largely composed of a number of hydrophobic residues that form part of the flap (residues 50–54) and the loop containing residues 80–83. The alternate S1–S3 binding site in the complex with (II) may be a preferable binding site from an energetics standpoint because of the hydrophobic nature of the P1–P3 group and is consistent with increased binding affinity of (II) over (I) for wild type [(II) has a K_i of 0.05 n*M* compared with 0.31 n*M* for (I)]. In the complex with (II), Arg8 of the protease is shifted somewhat and makes no contact with (II). Instead, it is involved in hydrogen bonding with the nearby water molecules (Fig. 2*c*). Besides the 80s loop of the monomer that is in direct contact with benzofuran group, the conformation of the rest of the protease main chain is similar to the structure of the complex of wild-type HIV-1 protease with (I). The two structures superimpose with an RMSD of 0.4 Å for 198 C^{α} pairs. Small conformational differences are also noticeable in the flap residues 49–53 of both the monomers of these two complexes. In order to make room for the benzofuran group, the C^{α} of Ile50 is displaced by 1.0 Å in the complex of (II) with wild-type protease. The binding mode for the benzofuran group and the large asymmetric shift of the 80s loop is impossible to envisage based on the structure of (I) with wild-type protease.

3.2. Structures of the 9X mutant protease–inhibitor complexes

The structure of the 9X mutant form of the protease complexed with (I) presents an unanticipated binding mode for the P1–P3 group and is similar to that observed for the complex of (II) with wild-type protease (Fig. 3*a*). In the complexes of (I) with the HIV-1 or HIV-2 wild type and with the 4X mutant of HIV-1 protease, the P1–P3 group points towards solvent and makes minimal contacts with the protease. However, in the complex with the 9X mutant HIV-1 protease, the P1–P3 group of (I), despite being a relatively small pyridyl moiety, is sandwiched between the 80s loop of one monomer and the flap and interacts with the alternate S1–S3 binding site. The 80s loop is pulled away from the active site in comparison with the complex of (I) with the wild-type HIV-1 protease. Residues 78–83 are displaced 0.6–2.89 Å, with Pro81 being displaced the most. Residues 48–53 of the flap, which interact with the P1–P3 group, are displaced by about 0.8 Å. Although the density for the P1–P3 group is weak, no significant electron density is found in the difference Fourier maps to justify the conformation of P1–P3 group to be as seen for the complex of (I) with wild-type protease. As in the case of the complex of (II) with wild-type protease, the conformational changes in the 80s loop are asymmetric, involving only the monomer that interacts with the P1–P3 group. The 80s loop for the second monomer shows no significant structural changes. The structures of the complexes of (I) with wild type and the 9X mutant protease of HIV-1 superimpose with an RMSD of 0.67 Å for 198 C^{α} pairs. Besides the P1–P3 group, the conformation of the rest of the inhibitor is conserved between the two complexes.

No significant conformational change in the 80s loop of the protease is observed in the complex of (III) with the 9X mutant protease compared with the complex of (III) with wild-type protease. Although electron density for the P1–P3 group of (III) is not well ordered in the complexes of (III) with 9X mutant, it seems to point towards the solvent just like the P1–P3 group of (III) in the wild-type complex (Fig. 3*b*). In the complex of (III) with wild-type protease, the P1–P3 group is also not well ordered (Munshi *et al.*, 1998). The complexes of (III) with the 9X mutant and with wild-type HIV-1 protease superimpose with an RMSD of 0.71 Å for 198 C^{α} pairs. Since the structure of P1–P3 could not be reliably defined in the structure, it has not been included in the refinement. The conformation of the rest of the inhibitor is conserved between the two complexes.

In the structure of the complex of the 9X mutant protease with (IV) (Saquinavir), the inhibitor appears to be bound in two different conformations that are related by the molecular dyad symmetry. A similar binding mode has been observed in the structure of the wild-type protease with (IV) (Krohn *et al.*, 1991). The 198 C^{α} pairs of the wild-type and 9X mutant complexes with (IV) superimpose with an RMSD of 0.65 Å. No significant structural differences are obvious between the structures of these two complexes. In particular, the conformation of the 80s loop for both subunits is not greatly perturbed (Fig. 3*c*). The 80s loop of both the monomers in the 9X mutant structure are pulled away in a symmetric fashion from the active site by about 0.5 Å. The inhibitor conformation is a conserved between the wild-type and 9X mutant protease complexes.

4. Discussion

4.1. Flexible 80s loop

Comparative analysis of the crystal structures of the complexes of (I) and (II) with wild type and of (I) with 9X mutant HIV-1 protease suggests that the P1–P3 group binds in two different S1–S3 binding sites. The P1–P3 group is flexible and its binding mode appears to be intimately coupled with the conformational state of the 80s loop. The structural flexibility of the P1–P3 group of analogs of (I) is partly reflected in the less well ordered electron density for these groups. In contrast, for the P1–P3 group of a different analog of (I) (L-840,236; data not shown) in the crystal structure of the complex with wild-type protease (K_i in the low nanomolar range) that binds in the same mode as (II), the electron density is well ordered. The P1–P3 group of this analog is largely hydrophobic and may bind tightly in the alternate S1–S3 binding site. Thus, depending upon the chemical nature, the P1–P3 group of some analogs of (I) may prefer either S1–S3 site, while others may dynamically interact with both. Superpositioning the structures of the wild-type protease with (I) and (II), and of 9X with (I) perhaps represents different

snapshots of this concerted structural rearrangement, involving the P1–P3 group of the inhibitor and the 80s loop (Fig. 4). Crystal packing does not appear to influence the conformation of the 80s loop, since the crystals of the complexes of wild-type protease with (I) and (II) belong to the same space group ($P2_12_12$) with similar lattice constants. On the other hand, despite different space groups and lattice constants between the crystals of the complexes of (III) or (IV) with the wild-type and 9X mutant protease, the conformation of the 80s loop and the inhibitor-binding mode is conserved. Crystals of the complexes of 9X with (III) or (IV) belong to the space group $P2_12_12_1$, whereas the crystals of wild type belong to $P2_12_12$ and $P6_1$, respectively.

4.2. Influence of mutations on the conformation of the 80s loop

The extent to which the mutations in the protease influence the conformation of the 80s loop is not clearly defined. The structure of the complex of (I) with the 4X mutant protease that contains Val82Thr and Ile84Val mutations in the vicinity of the 80s loop shows no significant conformational differences when compared with the structure of the complex of (I) with wild-type protease (Chen *et al.*, 1995; Schock *et al.*, 1996). On the other hand, in the complex of (I) with 9X mutant protease that contains only Val82Thr mutation in the active site, the binding mode of P1–P3 and the conformation of the 80s loop is altered. However, the contribution of the other eight non-active-site mutations towards the structural change is unclear. The asymmetric changes in the 80s loop have also been observed in the Val82Ala mutant HIV-1 protease in complex with A-77003 (Baldwin *et al.*, 1995) and in the complexes of SB203386 with different mutant forms of HIV-1 (Swairjo *et al.*, 1998). Inhibitor complexes with the HIV-2 protease have been reported

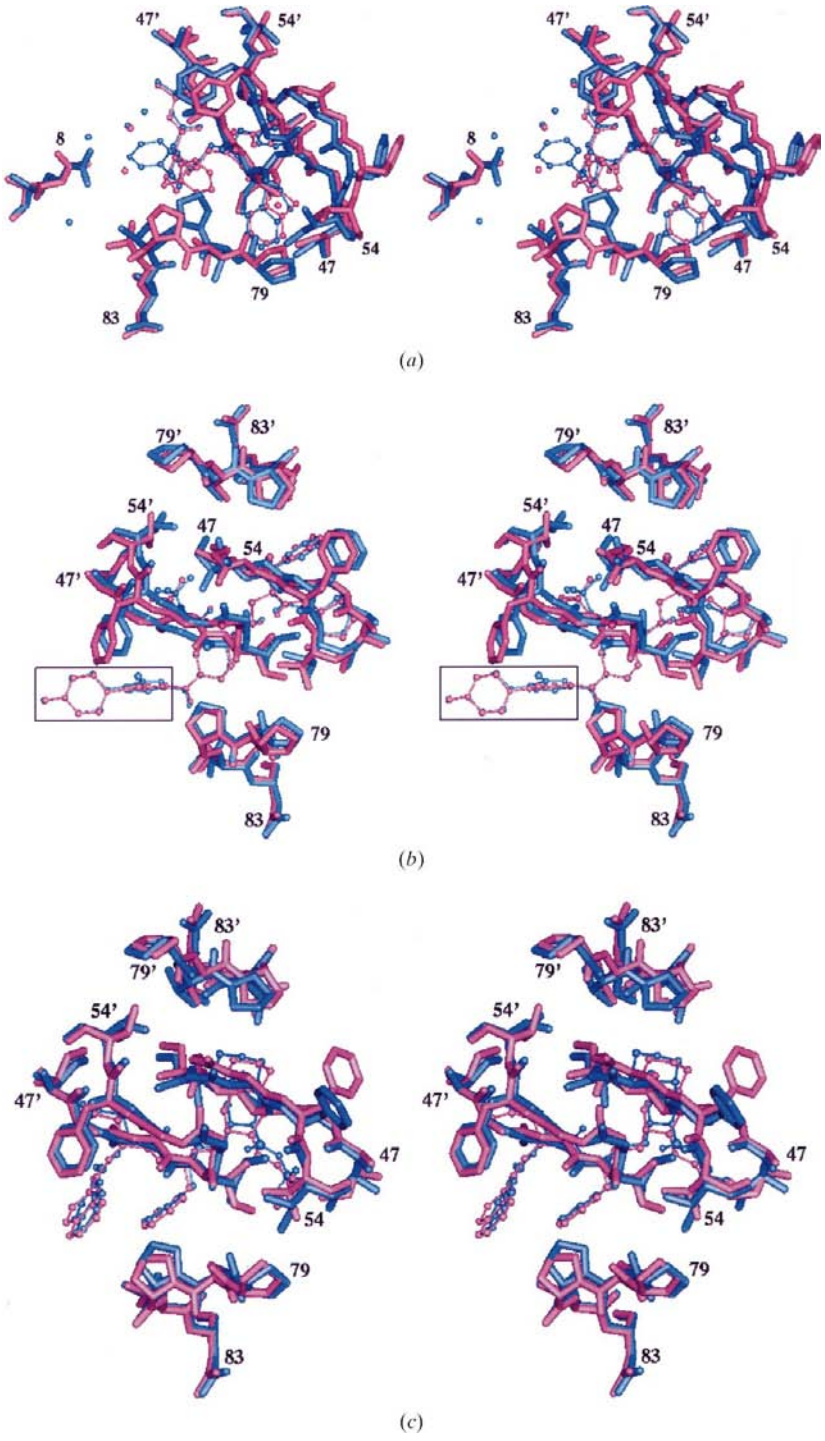

Figure 3
(*a*) Superposition of the crystal structures of (I) complexed with wild-type (blue) and with the 9X mutant HIV-1 protease (pink). The 80s loop, comprised of the residues 79–83, and the flap residues 47–54 are depicted. The inhibitor structures are represented as ball-and-stick models. The P1–P3 (pyridyl) of (I) occupies two different positions. In the 9X mutant complex, P1–P3 is sandwiched between the 80s loop and the flap and Pro81 is shifted as far as 2.8 Å in order to accommodate the P1–P3 group. Appropriately colored dots represent the water molecules in the two structures. (*b*) Superposition of the crystal structures of (III) complexed with the wild-type (blue) and with the 9X mutant HIV-1 protease (pink). The 80s loops and the flaps corresponding to two monomers are depicted. Enclosed in the box is the part of the inhibitor not well defined in the electron density. The conformations of the 80s loop and the flaps are not significantly altered between the two structures. (*c*) Superposition of the crystal structures of (IV) complexed with the wild-type (blue) and with the 9X mutant HIV-1 protease (pink). The 80s loops and the flaps corresponding to the two monomers are depicted. The conformations of the 80s loop and the flaps are not significantly altered between the two structures. Inhibitor binds in two modes that are related by the dyad symmetry of the dimer; however, for brevity, only one binding mode is depicted. No significant conformational changes are observed in the flaps or in the 80s loops between the two structures.

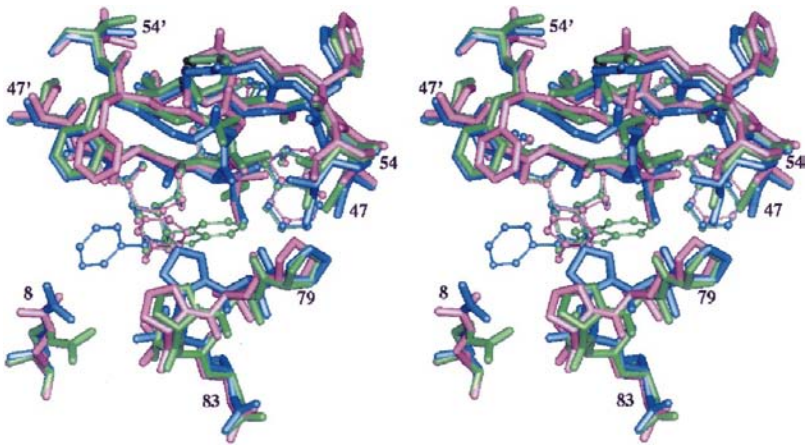

Figure 4
Superposition of the crystal structures of the wild-type (blue) and 9X mutant HIV-1 protease (pink) with (I) and that of (II) complexed with wild-type protease (green). The 80s loops and the flap are depicted. The inhibitor structures are represented as ball-and-stick models. The P1–P3 groups of (I) and (II) occupy three different positions in three different structures. Conformational changes in the 80s loop and the flaps are depicted.

with structural changes in the 80s loop when compared with the structures of these inhibitor complexes with the HIV-1 protease (Priestle *et al.*, 1995; Mulichak *et al.*, 1993). However, in contrast, no significant changes in the 80s loop have been observed between the complexes of (I) with the HIV-1 and HIV-2 protease or in the complexes of SB203386 with wild type and with a triple mutant (Val32Ile, Ile47Val, Val82Ile; Hoog *et al.*, 1996). Thus, it is not obvious to what extent the mutations influence the conformation around the active site. The eventual conformation in the complex may depend both on the chemical nature of the bound inhibitor and the enzyme form.

4.3. Alternate S1–S3 binding site

The alternate S1–S3 binding site is composed of residues Gly48, Gly49, Ile50, Val82 and Pro81. These residues provide a favorable environment for the hydrophobic benzofuran group of (II) [and other hydrophobic functional groups in various other analogs of (II)] and are involved in tight interactions with the inhibitor. It would not have been possible to rationally predict this binding site based on the structure of (I) with wild-type HIV-1 protease. The alternate S1–S3 binding site provides a unique opportunity for designing potent analogs of (II). The concerted nature of the flexibility of the 80s loop and the P1–P3 group of this inhibitor class may be exploited to design branched analogs that interact simultaneously with two S1–S3 binding sites. The alternate S1–S3 site also brings the P2′ group of these analogs in proximity of the P1–P3, thus even allowing the possible design of macrocyclic inhibitors.

5. Conclusions

The 80s loop of wild-type HIV-1 protease is intrinsically flexible. Depending upon the nature and the conformation of the bound inhibitor, the 80s loop can undergo concerted conformational changes in order to accommodate the inhibitor subgroups. Mutations in the amino acids of the protease are not essential for the observation of conformational changes in this loop and the influence of the mutations on the structure of the 80s loop is inhibitor dependent. The results presented also suggest that the structural changes observed are not a consequence of any crystal packing effects but are a reflection of the flexible nature of the protease. Other hot spots in the protease that are flexible have been suggested (Swairjo *et al.*, 1998; Freedberg *et al.*, 1998) and the virus may employ these features to its advantage. It is conceivable that some of the non-active-site mutations (Olsen *et al.*, 1999) influence the inhibitor/substrate binding by exploiting these flexible regions of the protease. Our results also suggest that the observed alternate binding pocket for the Indinavir analogs can be made available by design of the inhibitor.

We thank Dr Emilio Emini for his continued support and Ms Colleen McDonough for the synthesis of inhibitor (II).

References

Abdel-Meguid, S. S., Metcalf, B. W., Carr, T. J., Demarsh, P., DesJarlais, R. L., Fisher, S., Green, D. W., Ivanoff, L., Lambert, D. M., Murthy, K. H. M., Petteway, S. R., Pitts, W. J., Tomaszek, T. A., Winborne, E., Zhao, B., Dreyser, G. B. & Meek, T. D. (1994). *Biochemistry*, **33**, 11671–11677.

Ala, P. J., Huston, E. E., Klabe, R. M., Jadhav, P. K., Lam, P. Y. S. & Chang, C. H. (1998). *Biochemistry*, **37**, 15042–15049.

Baldwin, E. T., Bhat, T. N., Liu, B., Pattabiraman, N. & Erickson, J. W. (1995). *Nature Struct. Biol.* **2**, 244–249.

Boden, D. & Markowitz, M. (1998). *Antimicrob. Agents Chemother.* **42**, 2775–2783.

Brünger, A. T. (1993). *X-PLOR Version 3.1 Manual: A System for X-ray Crystallography and NMR*. New Haven, CT: Yale University Press.

Carroll, S. S. & Kuo, L. C. (1998). *Int. Antivir. News*, **6**(6), 103–107.

Chen, Z., Li, Y., Chen, E., Hall, D. L., Darke, P. L., Culberson, C., Shafer, J. A. & Kuo, L. C. (1994). *J. Biol. Chem.* **269**, 26344–26348.

Chen, Z., Li, Y., Schock, H. B., Hall, D. L., Chen, E. & Kuo, L. C. (1995). *J. Biol. Chem.* **270**, 21433–21436.

Condra, J. H. (1998). *Drug Resist. Updates*, **1**(5), 292–299.

Condra, J. H., Holder, D. J., Schleif, W. A., Blahy, O. M., Danovich, L. J., Gabryelski, D. J., Graham, D. L., Quintero, J. C., Rhodes, A., Robbins, H. L., Roth, E., Shivaprakash, M., Yang, T., Chodakewitz, J. A., Deutsch, P. J., Leavitt, R. Y., Massari, F. E., Mellors, J. W., Squires, K. E., Steigbigel, R. T., Teppler, H. & Emini, E. A. (1996). *J. Virol.* **70**(12), 8270–8276.

Freedberg, D. I., Wany, Y., Stahl, S., Kaufman, J. D, Wingfield, P. T., Kiso, Y. & Torchia, D. A. (1998). *J. Am. Chem. Soc.* **120**, 7916–7923.

Gulick, R. M., Mellors, J. W., Havlir, D., Eron, J. J., Gonzalez, C., McMahon, D., Jonas, L., Meibohm, A., Holder, D., Schleif, W. A., Condra, J. H., Emini, E. A., Isaacs, R., Chodakewitz, J. A. & Richman, D. D. (1998). *J. Am. Med. Assoc.* **280**(1), 35–41.

Gulick, R. M., Mellors, J. W., Havlir, D., Eron, J. J., Gonzalez, C., McMahon, D., Richman, D. D., Valentine, F. T., Jonas, L., Meibohm, A., Emini, E. A. & Chodakewitz, J. A. (1997). *New Engl. J. Med.* **337**(11), 734–739.

Hoog, S. S., Towlet, E. M., Zhao, B., Doyle, M. L, Debouck, C. & Abdel-Meguid, S. S. (1996). *Biochemistry*, **35**, 10279–10286.

Krohn, A., Redshaw, S., Ritchie, J., Graves, B. J. & Hatada, M. H. (1991). *J. Med. Chem.* **34**, 3340–3342.

Matthews, B. W. (1968). *J. Mol. Biol.* **33**, 491–497.

Molla, A., Korneyeva, M., Gao, Q., Vasavanonda, S., Schipper, P. J., Mo, H. M., Markowitz, M., Chernyavskiy, N. P., Lyons, N., Hsu, A., Granneman, G. R., Ho, D. D., Boucher, C. A. B., Leonard, J. M., Norbeck, D. W. & Kempf, D. J. (1996). *Nature Med.* **2**, 760–766.

Mulichak, A. M., Hui, J. O., Tomasselli, R. A., Heinrikson, R. L., Curry, K. A., Tomich, C. S., Thaisrivongs, S., Sawyer, T. K. & Watenpaugh, K. D. (1993). *J. Biol. Chem.* **268**, 13103–13109.

Munshi, S., Chen, Z., Li, Y., Olsen, D. B., Fraley, M. E., Hungate, R. W. & Kuo, L. C. (1998). *Acta Cryst.* D**54**, 1053–1060.

Olsen, D. B., Stahlhut, M. W., Rutkowski, C., Schock, H. B., vanOlden, A. L. & Kuo, L. C. (1999). *J. Biol. Chem.* **274**, 23699–23701.

Otwinowski, Z. & Minor, W. (1997). *Methods Enzymol.* **276**, 307–326.

Patick, A. K., Mo, H., Markowitz, M., Appelt, K., Wu, B., Musick, L., Kalish, V., Kaldor, S., Reich, S., Ho, D. & Webber, S. (1996). *Antimicrob. Agents Chemother.* **40**, 292–297.

Priestle, J. P., Fassler, A., Rosel, J., Tintelnot-Blomley, M., Strop, P. & Grutter, M. G. (1995). *Structure*, **3**, 381–389.

Ridky, T. W., Kikonyogo, A., Leis, J., Gulnik, S., Copeland, T., Erickson, J. W., Wlodawer, A., Kurinov, I., Harrison, R. W. & Weber, I. T. (1998). *Biochemistry*, **37**, 13835–13845.

Schock, H. B, Garsky, V. M. & Kuo, L. C. (1996). *J. Biol. Chem.* **271**, 31957–31963.

Smith, T. & Swanstrom, R. (1996). *Antivir. Ther.* **1**(1), 12–13.

Stebbins, J., Towler, E. M., Tennant, M. G., Deckman, I. C. & Debouck, C. (1997). *J. Mol. Biol*, **267**(3), 467–475.

Swairjo, M. A., Towler, E. M., Debouck, C. & Abdel-Meguid, S. S. (1998). *Biochemistry*, **37**, 10928–10936.

Tisdale, M., Myers, R. E., Maschera, B., Parry, N. R., Oliver, N. M. & Blair, E. D. (1995). *Antimicrob. Agents Chemother.* **39**, 1704–1710.

Wlodawer, A. & Erickson, J. W. (1993). *Annu. Rev. Biochem.* **62**, 543–585.

Wlodawer, A. & Vondrasek, J. (1998). *Annu. Rev. Biophys. Biomol. Struct.* **27**, 249–284.